

Asteroseismic model fitting by comparing $\epsilon_{n\ell}$ values

Ian W. Roxburgh

Astronomy Unit, Queen Mary University of London, Mile End Road, London E1 4NS, UK
 e-mail: I.W.Roxburgh@qmul.ac.uk

Received 25 May 2015 / Accepted 26 October 2015

ABSTRACT

We present an asteroseismic model fitting algorithm based on comparing model and observed $\epsilon_\ell(\nu)$ values defined in terms of frequencies by $\nu_{n\ell} = \Delta [n + \ell/2 + \epsilon_\ell(\nu_{n\ell})]$ where Δ is an average large separation. We show that if two stellar models have the same interior structure but different outer layers then the difference between their $\epsilon_\ell(\nu)$ values, interpolated to the same frequencies, collapses to a function only of frequency, independent of angular degree ℓ . The algorithm tests the goodness fit by comparing the difference in model and observed ϵ values after having subtracted off a best fit ℓ independent function of frequency $\mathcal{F}(\nu)$, and only requires interpolation in model values and not in observed values so the errors on the observed values are uncorrelated; it is independent of the n values assigned to the radial ordering of the frequencies and does not require the calculation of inner phase shifts of the model. We contrast this to a proposed direct frequency matching technique which minimises the difference between observed and model frequencies after having subtracted off an ℓ independent fit to these differences. We show this technique is flawed in principle, that all models with the same dimensionless structure but any mass and radius have the same quality of fit to an observed data set, and that it can give erroneous best fit models. We illustrate the epsilon matching technique by comparing stellar models and then apply it to data on HD 177153 (aka Perky). On comparing observations with a set of main sequence evolutionary models we find that models which satisfy constraints on the luminosity, radius, Δ , and on ϵ matching, have masses in the range $1.155 \pm 0.035 M_\odot$ and ages in the range $4.486 \pm 0.250 \times 10^9$ yr. Since the large separation and the radius are surface layer dependent we examine “pure surface layer independent” model fitting where the only constraints on the model fitting are on the luminosity and epsilon matching, and show that the best fit models have $M/M_\odot = 1.13 \pm 0.06$ and age = $4.62 \pm 0.39 \times 10^9$ yr.

Key words. stars: oscillations – asteroseismology – stars: interiors – methods: analytical – methods: numerical

1. Introduction

The seemingly straight forward way to find a model that has the same internal structure as an observed star is to seek to match the model and observed frequencies. The problem that besets such an approach is that it requires accurate modelling of the outer layers of a star, since these layers make a significant contribution to the values of the frequencies. However our understanding of the physics of these layers is poor, e.g. modelling convection, the equation of state, diffusion/levitation, mixing..., which renders it difficult to reliably model these outer layers.

In previous papers we have presented two model fitting techniques which overcome this difficulty by seeking to subtract off the unknown contribution of the outer layers and just fit the interior structure: comparison of the ratio of small to large separations (Roxburgh & Vorontsov 2003a, 2013; Roxburgh 2005) and phase matching (Roxburgh & Vorontsov 2003b; Roxburgh 2015a). The former suffers from having to interpolate in the observed frequencies and from correlation of errors, the latter from having to calculate inner phase shifts of the stellar models.

We here present a technique based on the result that if a star and a model have the same interior structure then the difference between their $\epsilon_\ell(\nu)$ values, evaluated at the same frequencies, collapses to a function only of frequency and not of angular degree ℓ . The ϵ are defined in terms of frequencies $\nu_{n\ell}$ by $\nu_{n\ell} = \Delta(n + \ell/2 + \epsilon_{n\ell})$ where Δ is an average large separation.

This procedure only requires knowledge of observed and model frequencies, and interpolates only in model frequencies so the errors on observational values are uncorrelated.

2. Properties of the frequencies and $\epsilon_{n\ell}$

A set of frequencies $\nu_{n\ell}$ of a (slowly rotating) main-sequence star can be represented in terms of “phases” $\epsilon_{n\ell}$ as

$$\nu_{n\ell} = \Delta [n + \ell/2 + \epsilon_{n\ell}] \quad \text{so} \quad \epsilon_{n\ell} = \epsilon_\ell(\nu_{n\ell}) = \frac{\nu_{n\ell}}{\Delta} - n - \ell/2 \quad (1)$$

where Δ is some arbitrarily chosen reference large separation usually taken as an average value $\Delta = \langle \nu_{n\ell} - \nu_{n-1,\ell} \rangle$. For a given Δ the $\epsilon_\ell(\nu)$ are therefore known at the discrete set of frequencies $\nu_{n\ell}$, but clearly their values depend the choice of Δ . An example is given in Fig. 1 for Model A of mass $1.15 M_\odot$, with 14 $\ell = 0, 1, 2$ frequencies in the range 1500–3000 μHz with an average large separation $\Delta = 104.3 \mu\text{Hz}$.

Model A, and all other models used in this paper, were calculated using the STAROX code (cf. Roxburgh 2008a), with EOS5 equation of state (Rogers & Nayfonov 2002), NACRE reaction rates (Angulo et al. 1999), OPAL/Whichita opacities (Iglesias & Rogers 1996; Ferguson et al. 2005), GS98 relative abundances (Grevesse & Sauval 1998), the mixing length model of convection, an Eddington atmosphere out to an optical depth of 10^{-3} , and do not include diffusion or convective overshooting. Frequencies were calculated using the OSCROXL code

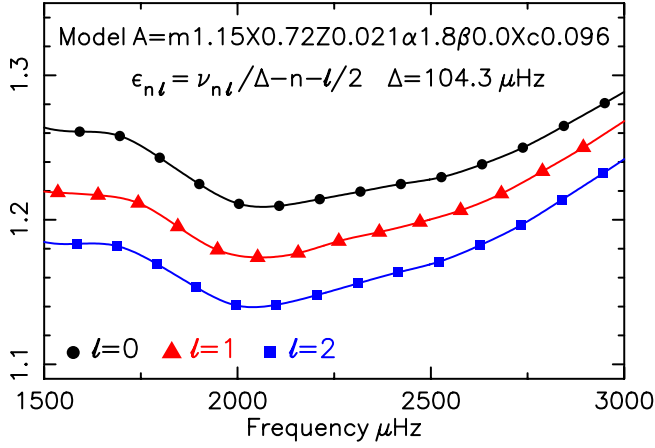


Fig. 1. $\epsilon_{n\ell}$ values for the frequencies of a main-sequence model of $1.15 M_{\odot}$ (Model A). The continuous curves $\epsilon_{\ell}(\nu)$ are obtained by interpolation in the discrete values.

(Roxburgh 2008b). Model A has an initial hydrogen abundance $X = 0.72$, heavy element abundance $Z = 0.021$, mixing length parameter $\alpha = 1.8$, no core overshooting ($\beta = 0$), and is evolved to a central hydrogen abundance $X_c = 0.096$ at an age of 4.6×10^9 yr.

The $\epsilon_{n\ell}$ measure the departure of the structure of a model from that of a uniform sphere and are determined by integrals over the structure of the star, the dominant contributions coming from the outer layers and the deep interior. As shown in previous work (cf. Roxburgh & Vorontsov 1994, 2000, 2013; Roxburgh 2015a, and references therein) these two contributions can be separated by solving the equations governing the oscillations of a star in terms of inner phase shifts $\delta_{\ell}(\nu, t)$ which satisfy the central boundary conditions and are determined by the structure of the inner layers, and outer phase shifts $\alpha_{\ell}(\nu, t)$ which satisfy the outer boundary conditions and are determined by the structure of the outer layers, where t is the acoustic radius $\int dr/c$. Both $\alpha_{\ell}(\nu, t)$ and $\delta_{\ell}(\nu, t)$ are continuous functions of both t and ν . The eigenfrequencies $\nu_{n\ell}$ are determined by continuity of the solutions at any arbitrarily chosen t and satisfy the eigenfrequency equation (Roxburgh & Vorontsov 2000)

$$\nu_{n\ell} = \Delta_T \left[n + \ell/2 + \alpha_{\ell}(\nu_{n\ell}, t) - \delta_{\ell}(\nu_{n\ell}, t) \right], \quad \Delta_T = \frac{1}{2T} \quad (2)$$

where T is the total acoustic radius of the star.

The important properties of this phase shift representation, on which all surface layer independent model fitting techniques rest, is that in the outer layers of a star, the outer phase shifts $\alpha_{\ell}(\nu, t)$ are almost independent of ℓ and beneath the near surface layers are almost independent of t , and can therefore be replaced by a single ℓ independent function $\alpha(\nu)$. This is illustrated in Fig. 2 where we plot the $\alpha_{\ell}(\nu, t)$ for Model A against acoustic radius t for 3 values of the frequency ν ; the curves for $\ell = 0, 1, 2$ at a given ν lie on top of each other until deep inside the star. The inner phase shifts are dependent on ℓ but are almost constant independent of acoustic radius in the outer layers beneath the near surface layers. (For a detailed analysis see Roxburgh 2015a.)

Suppressing the matching radius t , which can be anywhere in the outer layers, Eq. (2) can be written in the form

$$\nu_{n\ell} = \Delta_T \left[n + \ell/2 + \epsilon_{\ell}(\nu_{n\ell}) \right], \quad \epsilon_{n\ell} = \epsilon_{\ell}(\nu_{n\ell}) = \alpha(\nu_{n\ell}) - \delta_{\ell}(\nu_{n\ell}). \quad (3)$$

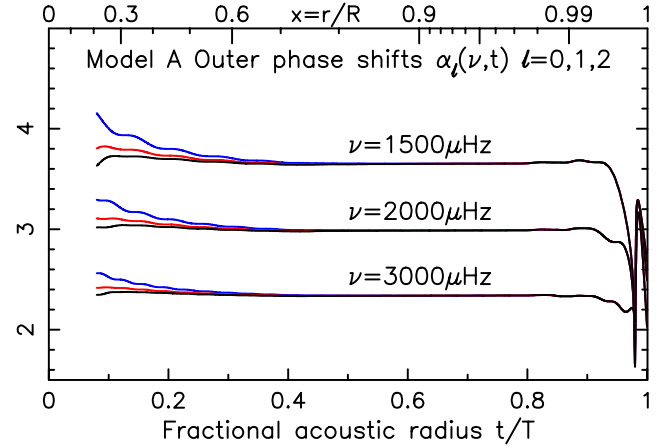


Fig. 2. Superposed curves for inner phase shift differences $\delta_{\ell 0}$ from the model, ϵ differences $\epsilon_{0\ell}(\nu)$ from interpolation in the $\epsilon_{n\ell}$ values from the frequencies, and the separation ratios r_{010}, r_{02} for Model A.

The surface phase shift, and hence the contribution of the outer layers, can be eliminated by interpolating the $\epsilon_{\ell}(\nu)$ values to the same frequency and subtracting so that

$$\epsilon_0(\nu) - \epsilon_{\ell}(\nu) = [\alpha(\nu) - \delta_0(\nu)] - [\alpha(\nu) - \delta_{\ell}(\nu)] = \delta_{\ell}(\nu) - \delta_0(\nu) \quad (4)$$

which only depend on the inner phase shift differences and hence on the inner structure of the star. The separation ratios (interpolated to the same frequency) are an approximation to these differences (cf. Roxburgh & Vorontsov 2003a,b, 2013).

Equation (3) relates the $\epsilon_{n\ell}$ to the value of the acoustic Δ_T but it can readily be transformed to any other chosen reference large separation Δ ; suppressing the fitting radius t and taking $\alpha_{\ell}(\nu) = \alpha(\nu)$ independent of ℓ in Eq. (2), we have

$$\nu_{n\ell} = \Delta \left[n + \ell/2 + \alpha(\nu_{n\ell}) - \delta_{\ell}(\nu_{n\ell}) \right] + \nu_{n\ell} \left[1 - \frac{\Delta}{\Delta_T} \right] \quad (5)$$

and since $\nu_{n\ell} [1 - \Delta/\Delta_T]$ is a function only of ν it can be absorbed into $\alpha(\nu)$; setting

$$\alpha^*(\nu, t) = \alpha(\nu, t) + \nu \left[\frac{1}{\Delta} - \frac{1}{\Delta_T} \right] \quad (6)$$

we have (on dropping the asterisk),

$$\nu_{n\ell} = \Delta \left[n + \ell/2 + \epsilon_{\ell}(\nu_{n\ell}) \right], \quad \epsilon_{\ell}(\nu_{n\ell}) = \alpha(\nu_{n\ell}) - \delta_{\ell}(\nu_{n\ell}). \quad (7)$$

The inner phase shifts $\delta_{\ell}(\nu)$ as a function of ν , which are determined by the inner structure of the star, are unchanged by this redefinition of α .

3. Models with the same interior structure

Consider 2 models with frequencies $\nu_{n\ell}^o, \nu_{n\ell}^m (\neq \nu_{n\ell}^o)$, with the same interior structure but different outer layers; their ϵ values at their frequencies in terms of inner and outer phase shifts are

$$\epsilon_{\ell}^o(\nu_{n\ell}^o) = \left[\nu_{n\ell}^o / \Delta^o - n - \ell/2 \right] = \left[\alpha^o(\nu_{n\ell}^o) - \delta_{\ell}^o(\nu_{n\ell}^o) \right] \quad (8a)$$

$$\epsilon_{\ell}^m(\nu_{n\ell}^m) = \left[\nu_{n\ell}^m / \Delta^m - n - \ell/2 \right] = \left[\alpha^m(\nu_{n\ell}^m) - \delta_{\ell}^m(\nu_{n\ell}^m) \right]. \quad (8b)$$

If the two models have the same interior structure then their inner phase shifts $\delta_{\ell}(\nu)$ as a function of ν are identical but are evaluated

at different frequencies $\nu_{n\ell}^m, \nu_{n\ell}^o$. If we interpolate in the values $\epsilon_\ell^m(\nu_{n\ell}^m)$ to determine the values at the frequencies $\nu_{n\ell}^o$ then

$$\epsilon_\ell^m(\nu_{n\ell}^o) = \alpha^m(\nu_{n\ell}^o) - \delta_\ell^m(\nu_{n\ell}^o) \quad (9a)$$

$$\epsilon_\ell^o(\nu_{n\ell}^o) = \alpha^o(\nu_{n\ell}^o) - \delta_\ell^o(\nu_{n\ell}^o). \quad (9b)$$

Since the two models have the same interior structure the inner phase shifts $\delta_\ell^m(\nu_{n\ell}^o) = \delta_\ell^o(\nu_{n\ell}^o)$, subtracting Eq. (9b) from Eq. (9a) gives

$$\mathcal{E}(\ell, \nu) = \epsilon_\ell^m(\nu_{n\ell}^o) - \epsilon_\ell^o(\nu_{n\ell}^o) = \alpha^m(\nu_{n\ell}^o) - \alpha^o(\nu_{n\ell}^o) = \mathcal{F}(\nu_{n\ell}^o) \quad (10)$$

where $\mathcal{F}(\nu)$ is an ℓ independent function of frequency.

So if the two models have the same interior structure then the difference in their ϵ values evaluated at the same frequency $\mathcal{E}(\ell, \nu)$ collapses to an ℓ independent function of frequency, whereas if they do not have the same interior structure then their differences are a function of both ℓ and ν . This is the basis of the model fitting algorithm presented here.

4. Model fitting algorithm

Given a set of observed frequencies $\nu_{n\ell}^o$ with error estimates $\sigma_{n\ell}$ and the frequencies $\nu_{n\ell}^m$ of a model, calculate their $\epsilon_\ell(\nu_{n\ell})$ and interpolate in $\epsilon_\ell^m(\nu_{n\ell}^m)$ to find the model values at the observed frequencies $\epsilon_\ell^m(\nu_{n\ell}^o)$ (e.g. by cubic spline interpolation). Then form their differences

$$\mathcal{E}(\ell, \nu_{n\ell}^o) = \epsilon_\ell^m(\nu_{n\ell}^o) - \epsilon_\ell^o(\nu_{n\ell}^o) \quad (11)$$

make an M parameter ℓ independent fit $\mathcal{F}(\nu)$ to $\mathcal{E}(\ell, \nu)$ (e.g. by a series in Chebychev polynomials $\sum C_k T_k(\nu)$, or in terms of basis B-splines) and determine the goodness of fit by the reduced χ^2

$$\chi^2 = \frac{1}{N - M} \sum_1^N \left(\frac{\mathcal{E}(\ell, \nu_{n\ell}^o) - \mathcal{F}(\nu_{n\ell}^o)}{s_{n\ell}} \right)^2. \quad (12)$$

The errors $s_{n\ell}$ are the errors in $\epsilon_\ell^o = \sigma_{n\ell} / \Delta^o$ where the $\sigma_{n\ell}$ are the errors on the observed frequencies and Δ^o the large separation of the observed frequencies. N is the total number of observed frequencies and M is the number of parameters in $\mathcal{F}(\nu)$ which minimises the χ^2 , subject to being less than the number of $\ell = 0$ frequencies.

This algorithm does not require one to determine the inner and outer phase shifts, only to interpolate in the model's ϵ_ℓ values which are known over a wide range of frequencies (minimising end effects in interpolation), and the errors $s_{n\ell}$ are uncorrelated.

5. Model examples

The first example is to compare Model A, (designated as the ‘‘observed’’ star) with frequencies $\nu_{n\ell}^o$ and error estimates $\sigma_{n\ell} = 0.15 \mu\text{Hz}$, with Model G, with frequencies $\nu_{n\ell}^m$, which has the same interior structure as Model A but is modified in the outer layers by setting Γ_1 constant above $r = 0.95R$; their frequency differences are shown in Fig. 3. In the top panel of Fig. 4 we show the $\epsilon_{n\ell}^m$ for Model G over a wider range of frequencies than the ‘‘observed’’ set, and their continuous curves $\epsilon_\ell(\nu)$ obtained by cubic spline interpolation. The interpolated values at the observed frequencies are marked by the crosses.

The residuals $\mathcal{E}(\ell, \nu_{n\ell}^o) - \mathcal{F}(\nu)$ of the fit to a function only of ν are shown in the bottom panel; with error estimates on the ‘‘observed’’ frequencies of $0.15 \mu\text{Hz}$ the reduced $\chi^2 = 0.016$, the

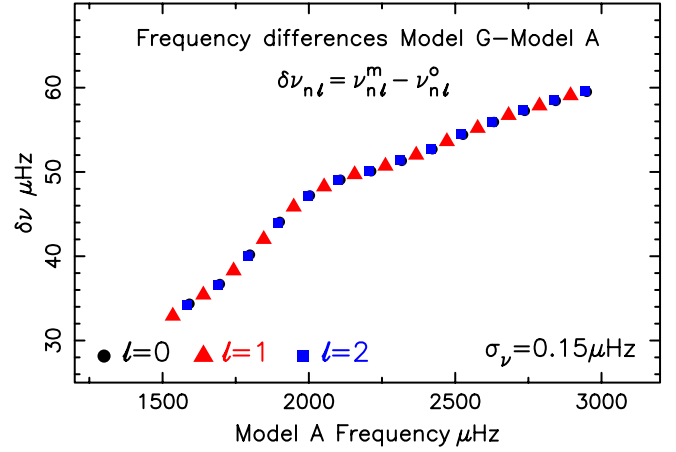


Fig. 3. Superposed curves for the outer phase shifts $\alpha_\ell(\nu, t)$ of Model A at 3 frequencies. The values of α_ℓ are independent of ℓ until deep inside the star.

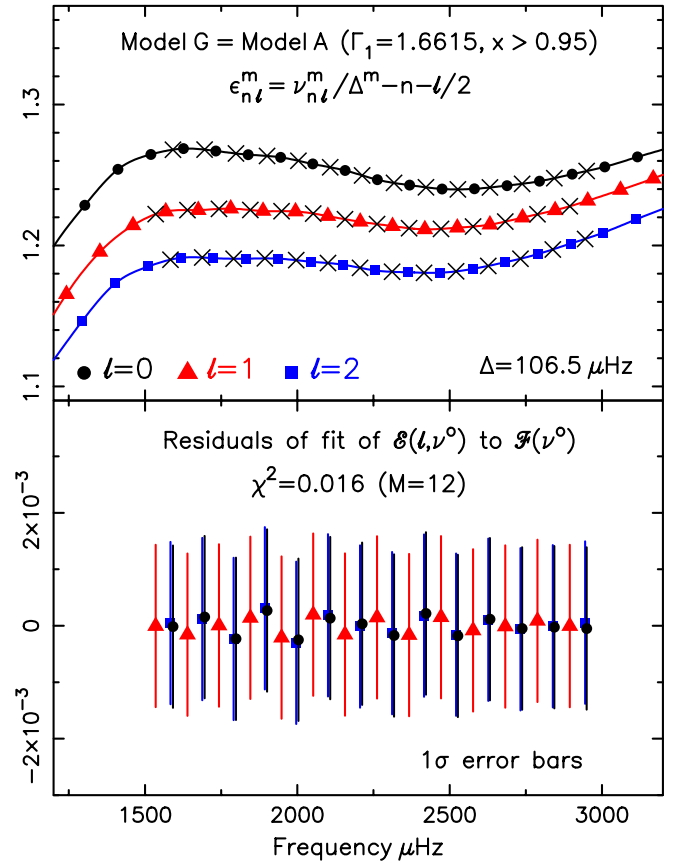


Fig. 4. *Top panel:* $\epsilon_{n\ell}^m$ for Model G, continuous curves $\epsilon_\ell(\nu)$ and interpolated values for $\epsilon_\ell^m(\nu_{n\ell}^o)$ at the ‘‘observed’’ frequencies of Model A (crosses). *Bottom panel:* residuals of fit of $\mathcal{E}(\ell, \nu_{n\ell}^o) = \epsilon_\ell^m(\nu_{n\ell}^o) - \epsilon_\ell^o(\nu_{n\ell}^o)$ to function of frequency $\mathcal{F}(\nu)$.

departure from zero being primarily due to errors in interpolation, and the fact that the outer layer contribution is not exactly independent of ℓ .

Our second example is to take a model similar to Model A and test how well it fits the epsilon values of model A. This model (Model B) has a mass of $1.13 M_\odot$, $XH = 0.70$, $Z = 0.022$, $\alpha = 1.8$, $X_c = 0.047$ and an age of 4.52×10^9 yr. The top panel in Fig. 5 shows the ϵ values for the model and the values in interpolated at the frequencies of Model A, and the bottom panel

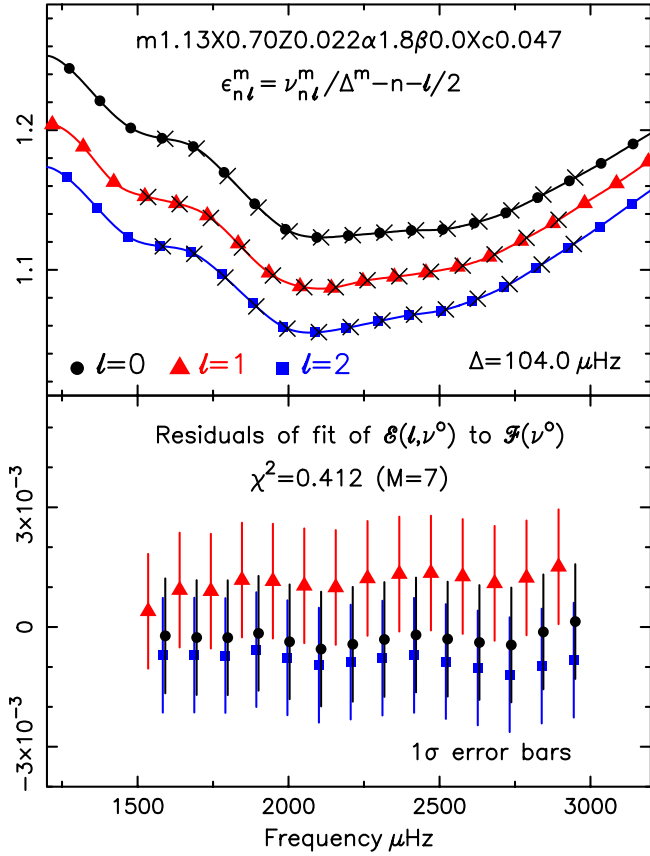


Fig. 5. Top panel: ϵ_{nl}^m for Model B, continuous curves $\epsilon_l(\nu)$ and interpolated values for $\epsilon_l^m(\nu_{nl}^o)$ at the “observed” frequencies of Model A (crosses). Bottom panel: residuals of fit of $\mathcal{E}(l, \nu_{nl}^o) = \epsilon_l^m(\nu_{nl}^o) - \epsilon_l^o(\nu_{nl}^o)$ to function of frequency $\mathcal{F}(\nu)$.

the residuals to the fit to of the ϵ differences to a function only of frequency. With error estimates on the frequencies of model A of $0.15 \mu\text{Hz}$ and $N - M = 35$ degrees of freedom, the χ^2 of the fit is 0.412 which corresponds to a probability of matching of 0.999; this model fits the ϵ values of Model A.

The results in Fig. 5 illustrate the fact that ϵ matching and separation ratios are not exactly equivalent. The points in Fig. 5 are the ϵ differences $(\epsilon_l^m - \epsilon_l^o) - \epsilon^{av}$ where $\epsilon^{av} = \mathcal{F}(\nu_l^o)$, whereas the difference between model and observed separation ratios is $(\epsilon_0^m - \epsilon_0^o) - (\epsilon_l^m - \epsilon_l^o)$ at ν_0^o . The resulting χ^2 for the two procedures are not in general the same, which is the smaller depends on the particular model and observed frequencies. In this example $\chi_{\text{ratios}}^2 = 0.506$ whereas from ϵ matching $\chi^2 = 0.412$.

The third model to be tested (Model C) has a mass of $1.15 M_\odot$ with $XH = 0.70$, $Z = 0.019$, $\alpha = 2.4$, $X_c = 0.200$ and an age of 3.6×10^9 yr. The top panel in Fig. 6 shows the ϵ values for this model and the values interpolated at the frequencies of Model A, and the bottom panel the residuals of the fit of the ϵ differences to a function only of frequency. With error estimates on the frequencies of model A of $0.15 \mu\text{Hz}$; the χ^2 of the fit is 3.16 which corresponds to a probability of matching of 3×10^{-9} , this model does not fit the ϵ values of Model A.

6. Model fitting by comparing frequencies rather than ϵ values

A seemingly simple alternative model fitting algorithm is to compare observed and model frequencies after having subtracted

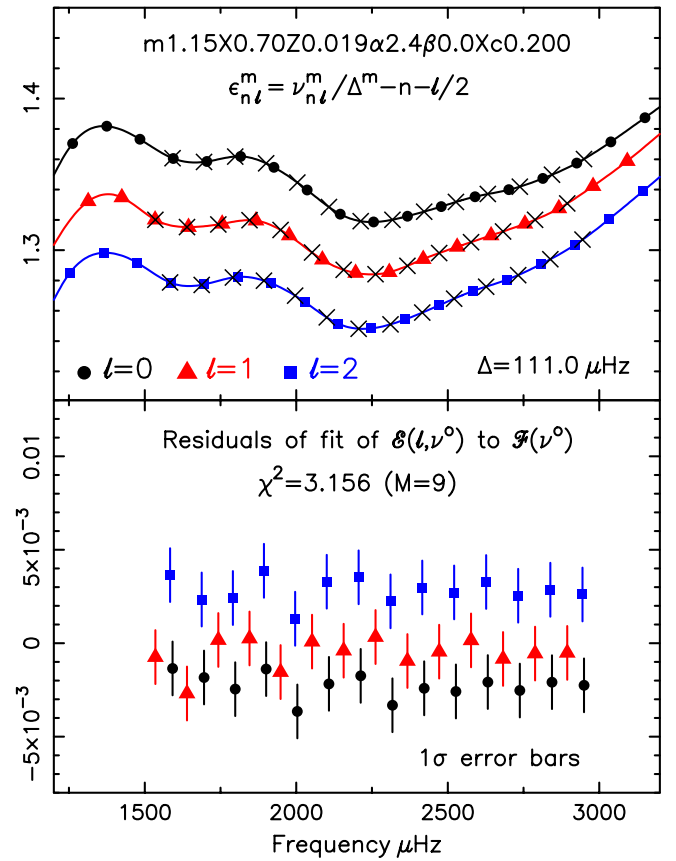


Fig. 6. Top panel: ϵ_{nl} values of the model C, the continuous curves $\epsilon_l(\nu)$ obtained by interpolation, and the values at the frequencies ν^o of Model A (the crosses). Bottom panel: residuals of fit of $\mathcal{E}(l, \nu_{nl}^o) = \epsilon_l^m(\nu_{nl}^o) - \epsilon_l^o(\nu_{nl}^o)$ to a function of frequency $\mathcal{F}(\nu)$. The χ^2 of the fit is 3.16, demonstrating that this model does not have the same interior structure as model A.

off an ℓ independent best fit $\mathcal{F}(\nu^o)$ to the frequency differences $\nu_{nl}^m - \nu_{nl}^o$, defining the goodness of fit χ_ν^2 as

$$\chi_\nu^2 = \frac{1}{N - M} \sum_1^N \left(\frac{\nu_{nl}^m - \nu_{nl}^o - \mathcal{F}(\nu^o)}{\sigma_{nl}} \right)^2 \quad (13)$$

where, as in ϵ matching, N is the number of frequencies and M the number of parameters in the function of frequency $\mathcal{F}(\nu)$. This was proposed as an alternative to the use of the surface layer offset approach advocated by Kjeldsen et al. (2008), with the offset determined as part of the fitting process rather than by scaling the solar value (cf. Roxburgh 2009). This was misguided as I show below!

Consider a (homologous) family of stellar models, that is a family with different masses M , and radii R , but the same dimensionless structure $q(x)$, $s(x)$, $p(x)$, $\Gamma_1(x)$, where $x = r/R$ and

$$M(r) = q(x)M, \quad \rho(r) = s(x) \frac{3M}{4\pi R^3}, \quad P(r) = p(x) \frac{3GM^2}{4\pi R^4}. \quad (14)$$

This family of models all have the same dimensionless frequencies ω_{nl} and the same inner phase shifts $\delta_\ell(\omega_{nl})$ as a function of dimensionless frequency, but the physical values of the frequencies differ since they are given by

$$\nu_{nl} = \left(\frac{GM}{R^3} \right)^{1/2} \omega_{nl} \quad (15)$$

the frequencies of any one model in the set being simply a linear scaling of those of any other model in the set.

Now if we have a model whose frequencies $\nu_{n\ell}^m$ satisfy the matching condition in Eq. (13), then so do all other members of the homology set since the difference in frequencies between any such models is simply a linear function of frequency and is therefore absorbed into $\mathcal{F}(\nu)$ in Eq. (13), giving the same χ^2 for all models in the set. So the frequency fitting algorithm (Eq. (13)) is not able to distinguish between stars with widely different M , R , which have the same dimensionless interior structure. The same problem applies to comparing separation ratios at the same radial order n , since the ratios – being ratios – are independent of a constant scaling on the frequencies.

This is not the case for the epsilon matching since we compare values at the same physical frequency. nor for comparison of separation ratios at the same frequency. There is one well known exception; all scaled models that have the same M/R^3 have the same physical frequency and asteroseismology alone cannot differentiate between this set of models.

Moreover the frequency matching algorithm Eq. (13) cannot, in principle, give a $\chi^2 = 0$ even if the model and observed star have the same interior structure, unless the model and observed frequencies, $\nu_{n\ell}^m, \nu_{n\ell}^o$, are a perfect match. From Eq. (5) we have

$$\nu_{n\ell}^m - \nu_{n\ell}^o = \Delta^o \left[\delta_\ell^o(\nu_{n\ell}^o) - \delta_\ell^m(\nu_{n\ell}^m) \right] + \mathcal{V}(\nu) \quad (16)$$

where $\mathcal{V}(\nu)$ is a function only of frequency given by

$$\mathcal{V}(\nu) = \Delta^o \left[\alpha^m(\nu_{n\ell}^m) - \alpha^o(\nu_{n\ell}^o) \right] + \nu_{n\ell}^m \left[1 - \frac{\Delta^o}{\Delta^m} \right]. \quad (17)$$

If the observed star and model have the same interior structure then the inner phase shifts have the same functional form so $\delta^m(\nu) = \delta^o(\nu)$ at the same frequencies, but in general $\delta^o(\nu_{n\ell}^m) \neq \delta^o(\nu_{n\ell}^o)$ at different frequencies and the frequency differences $\nu_{n\ell}^m - \nu_{n\ell}^o$ are ℓ dependent, unless the observed and model frequencies are the same.

As an example of a spurious good fit from frequency matching we apply the algorithm (Eq. (13)) to model C whose ϵ matching residuals with a $\chi^2 = 3.16$ are shown in Fig. 6; the residuals from frequency fitting are shown in Fig. 7 and have a $\chi^2 = 0.77$, naively suggesting that model C is a good fit to Model A. This is not the case as can be seen from Fig. 7b where we plot the sound speed squared and density as a function of radial distance from the centre (in units 10^{11} cm).

However if the model is a good fit to the observations as determined by epsilon matching ($\chi_\epsilon^2 < 1$), it may, or may not, also have value of $\chi_\nu^2 < 1$, depending on whether or not the n values of the model and observed star are in agreement, or the change in the inner phase shifts δ_ℓ over a large separation is sufficiently small.

7. ϵ model fitting to HD 177153 (aka Perky)

The star HD 177153 (aka Perky) was observed by *Kepler* (KIC 6106415) and Silva Aguirre et al. (2013) list a total of 33 frequencies, 11 for each $\ell = 0, 1, 2$, a $\nu_{\max} \sim 2210 \mu\text{Hz}$ and an average large separation $\Delta = 104.0 \pm 0.5 \mu\text{Hz}$.

Model fitting was undertaken by Silva-Aguirre et al. (2013) using two procedures: comparing frequencies with a ‘‘surface offset’’ (cf. Kjeldsen et al. 2008), and comparing separation ratios (cf. Roxburgh & Vorontsov 2003a, 2013); and more recently by Roxburgh (2015a) using the phase matching technique.

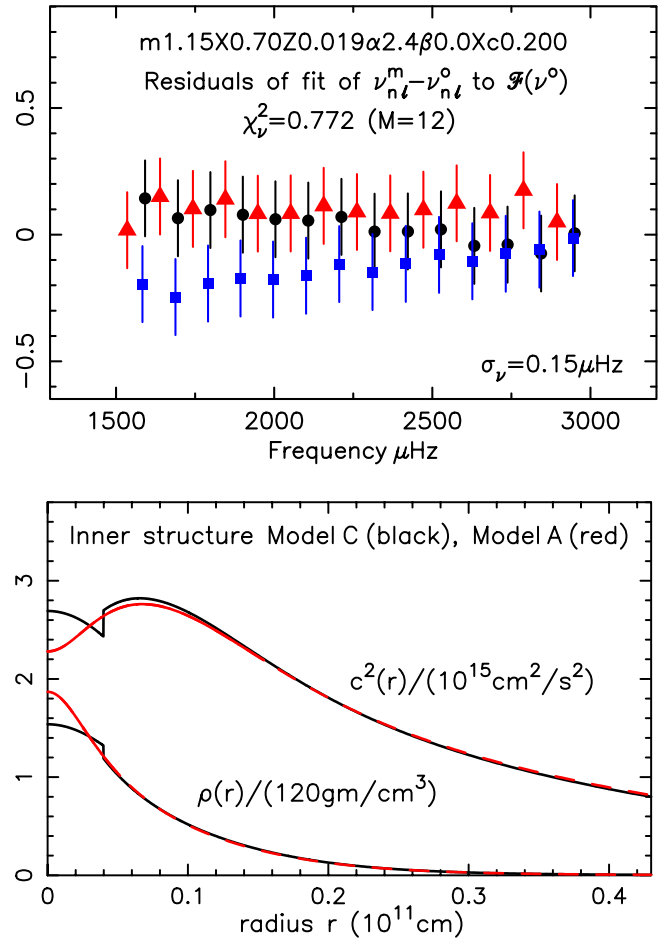


Fig. 7. Top panel: residuals of the fit of the frequencies of model C to those of Model A using the frequency matching algorithm (Eq. (13)) gives a $\chi_\nu^2 = 0.77$. Bottom panel: internal structure of the models.

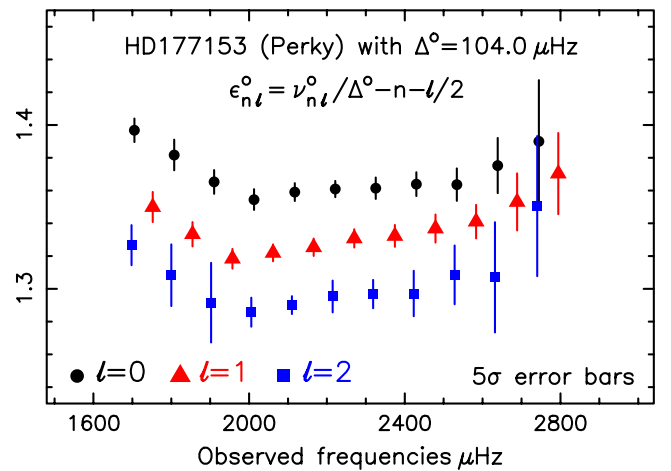


Fig. 8. $\epsilon_{n\ell}$ values of the observed frequencies of HD 177153 (aka Perky). The error bars shown are 5σ to enable them to be seen.

Here we apply the ϵ matching technique described above to the same star. The $\epsilon_{n\ell}$ values are displayed in Fig. 8 – note that the error bars have been multiplied by 5 in order that they can be seen.

As in Roxburgh (2015a) we take constraints on luminosity and radius derived from angular diameter and bolometric flux

Table 1. HD 177153: 1σ best fit models: $Y \geq 0.255$.

| M/M_{\odot} | L/L_{\odot} | R/R_{\odot} | XH | Z | α | X_c | age9 | Δ_{μ} | χ^2 |
|---------------|---------------|---------------|-------|-------|----------|-------|-------|----------------|----------|
| 1.120 | 1.843 | 1.254 | 0.709 | 0.020 | 1.670 | 0.095 | 4.540 | 103.3 | 1.110 |
| 1.130 | 1.823 | 1.253 | 0.710 | 0.021 | 1.700 | 0.097 | 4.562 | 103.8 | 0.974 |
| 1.140 | 1.800 | 1.254 | 0.704 | 0.023 | 1.712 | 0.101 | 4.433 | 104.2 | 0.940 |
| 1.150 | 1.821 | 1.260 | 0.710 | 0.023 | 1.726 | 0.102 | 4.465 | 103.9 | 0.910 |
| 1.150 | 1.871 | 1.253 | 0.720 | 0.021 | 1.800 | 0.096 | 4.601 | 104.2 | 0.859 |
| 1.160 | 1.880 | 1.257 | 0.710 | 0.023 | 1.800 | 0.098 | 4.275 | 104.2 | 1.001 |
| 1.160 | 1.829 | 1.254 | 0.710 | 0.024 | 1.800 | 0.095 | 4.449 | 104.6 | 0.960 |
| 1.160 | 1.869 | 1.259 | 0.720 | 0.022 | 1.800 | 0.096 | 4.572 | 104.4 | 0.865 |
| 1.160 | 1.812 | 1.255 | 0.720 | 0.023 | 1.800 | 0.099 | 4.736 | 104.6 | 1.014 |
| 1.170 | 1.883 | 1.263 | 0.710 | 0.024 | 1.800 | 0.097 | 4.236 | 104.3 | 1.041 |
| 1.170 | 1.869 | 1.266 | 0.720 | 0.023 | 1.800 | 0.095 | 4.538 | 104.0 | 0.885 |
| 1.170 | 1.815 | 1.261 | 0.720 | 0.024 | 1.800 | 0.097 | 4.701 | 104.2 | 1.040 |
| 1.180 | 1.869 | 1.271 | 0.720 | 0.024 | 1.800 | 0.099 | 4.484 | 103.8 | 0.916 |
| 1.190 | 1.810 | 1.275 | 0.714 | 0.027 | 1.772 | 0.102 | 4.456 | 103.7 | 1.067 |
| 1.150 | 1.825 | 1.247 | 0.710 | 0.023 | 1.800 | 0.097 | 4.486 | 105.0 | 0.937 |
| 1.100 | 1.835 | 1.253 | 0.710 | 0.018 | 1.600 | 0.096 | 4.630 | 102.5 | 1.071 |
| 1.110 | 1.830 | 1.260 | 0.710 | 0.019 | 1.600 | 0.095 | 4.627 | 102.1 | 1.038 |

measurements by Huber et al. (2012) and the revised HIPPARCOS parallax (van Leeuwen 2007) giving

$$L/L_{\odot} = 1.814 \pm 0.076 \quad R/R_{\odot} = 1.288 \pm 0.036.$$

We define an average large separation in terms of the frequencies, setting $\Delta = [\nu_{n+3,0} - \nu_{n-2,0}]/5$ where $\nu_{n,0} \leq \nu_{\max} < \nu_{n+1,0}$, since this can be applied to both observations and models, and take an error estimate of $1 \mu\text{Hz}$, larger than that given by Silva Aguirre et al. to allow for the uncertainty due to the relatively large contribution of the outer layers (Roxburgh 2014) and the fact that even in the solar case Δ from solar models differs from the observed value by $\sim 1 \mu\text{Hz}$; this gives an observational constraint of $\Delta^{\circ} = 104 \pm 1 \mu\text{Hz}$. Since we are using a surface layer independent model fitting algorithm it would be inconsistent to impose a constraint on the surface $[\text{Fe}/\text{H}]$ (which is anyway poorly constrained) and is unlikely to reflect the interior composition due to diffusion/levitation/mixing in the outer layers.

We searched for best fit models in just one model set with Grevesse & Sauval (1998) abundances computed using my STAROX code (Roxburgh 2008a) as described in Sect. 2 above. The model set has masses in the range $0.85\text{--}1.40 M_{\odot}$, initial hydrogen abundance XH in the range $0.68\text{--}0.74$, metal abundance Z in the range $0.014\text{--}0.026$, mixing length parameter α in the range $1.1\text{--}2.4$, and evolutionary models from the initial to terminal main sequence. These models do not include convective overshooting or diffusion/levitation.

We define best fit models as those that satisfy the luminosity, radius and large separation constraints to within 1σ , and which have $\chi^2 \leq 1.114$ for the epsilon fitting. The limit on χ^2 corresponds to a probability of 0.317 of being due to a random realisation of errors for $N - M = 24$ degrees of freedom (i.e. $N = 33$ frequencies and $M = 9$ parameters in the representation of $\mathcal{F}(\nu)$), the same as the 1σ limit for 1 degree of freedom. Likewise we set a 2σ limit on χ^2 of 1.535 corresponding to a probability of 0.0455, the same as the 2σ limit for 1 degree of freedom. One additional constraint can be added; namely that the initial Helium abundance (Y) should be greater than the initial helium fraction from the Big Bang; we set a lower limit on Y of 0.255

In Table 1 we give models that all fell with the 1σ limits; the models have masses in the range $1.155 \pm 0.035 M_{\odot}$ and ages in the range $4.486 \pm 0.250 \times 10^9$ yr (age9 is age in Gyr and Δ_{μ} the large separation in μHz); well within the target accuracy of 10% required for the PLATO mission (cf. Rauer et al. 2014). The first model below the line has a slightly small radius whilst the following two models are within 2σ for Δ – allowing for the fact that the value of Δ , and to a lesser extent the radius, are influenced by the structure of the outer layers of a star.

We have excluded models with low Helium abundance $0.234 \leq Y < 0.255$; however these models have similar masses and ages to those in Table 1 with $1.13 \leq M/M_{\odot} \leq 1.18$ and ages in the range $4.64\text{--}4.89 \times 10^9$ yr.

Figures 9 give the results for one of the best fit models which has $M = 1.15 M_{\odot}$, $XH = 0.72$, $Z = 0.021$, $\alpha = 1.8$, $X_c = 0.096$, an age of 4.6×10^9 yr. and $\Delta = 104.2 \mu\text{Hz}$. The upper panel shows the $\epsilon_{n\ell}$ values for this model, the points are the model values, the curves are the result of fitting a cubic spline through these model values, and the crosses the interpolated values at the observed frequencies. The bottom panel gives the residuals of the fit of the differences $\mathcal{E}(\ell, \nu) = \epsilon_{\ell}^{\circ}(\nu_{n\ell}^{\circ}) - \epsilon_{\ell}^m(\nu_{n\ell}^m)$ to a function $\mathcal{F}(\nu)$ only of frequency, which has a reduced $\chi^2 = 0.86$. This model has an interior structure compatible with that of the observed star HD 177153.

It is worth pointing out that the frequency offsets – that is the difference between the observed frequencies and those of the best fit models $\nu_{n\ell}^{\circ} - \nu_{n\ell}^m$, do not, in general, follow a Kjeldsen-like power law $a\nu^b$, and can be positive and/or negative. This is discussed in detail in Roxburgh (2015b). The one exception is the $1.150 M_{\odot}$ model below the line in Table 1 which does have a Kjeldsen-type offset (cf. Roxburgh 2015b).

8. Relaxing the constraints – pure surface layer independent model fitting

In the above we have followed the procedure generally used in model fitting, requiring models to satisfy observational constraints on luminosity, radius (or effective temperature) and large

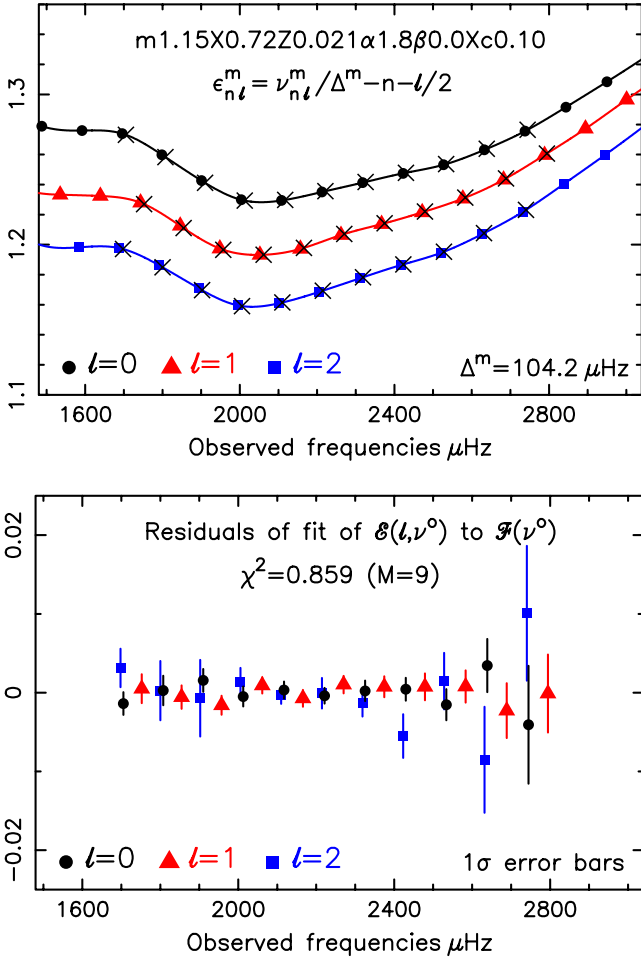


Fig. 9. *Top panel:* ϵ_{nl} values of a model of $1.15 M_{\odot}$, the crosses mark the interpolated values at the observed frequencies of HD 177153. *Bottom panel:* residuals of fit of $\mathcal{E}(\ell, \nu^o) = \epsilon_{\ell}^m(\nu_{nl}^o) - \epsilon_{\ell}^o(\nu_{nl}^o)$ to $\mathcal{F}(\nu^o)$, a function only of frequency.

separation, as well as fitting to the frequencies – here in the form of epsilon matching. But this is not actually surface layer independent model fitting. Whilst the luminosity L (and mass M) are essentially independent of the structure of the outer layers, being determined by the run of density, temperature and composition profiles in the fully ionised inner layers, the large separation Δ and radius R are strongly influenced by the structure of the outer layers which depend on the model of convection, diffusion and the equation of state in regions of ionisation. We therefore explore the consequences of relaxing constraints on Δ and R .

In Table 2 we give the results of such an analysis. An entry of 1 signifies that the constraint was imposed with a 1σ limit, ∞ that the constraint was not imposed, and 2 that the constraint was imposed with a 2σ limit. As mentioned above we take the 1σ limit for χ^2 as 1.114, and the 2σ limit as 1.535. The first row corresponds to the models in Table 1 where all variables L , R , Δ , χ^2 are within their 1σ limits; and rows 2–7 have different combinations of constraints on L , R , Δ and rows 8 and 9 have no constraint from ϵ matching. The last 3 rows below the line are for 2σ limits.

From the data in row 4 we see that “pure surface layer independent model fitting”, that is just imposing a 1σ constraint on the luminosity and on epsilon matching, is effective in narrowing down the range of possible models both in terms of age and mass giving $M/M_{\odot} = 1.13 \pm 0.06$ and age = $4.62 \pm 0.39 \times 10^9$ yr.

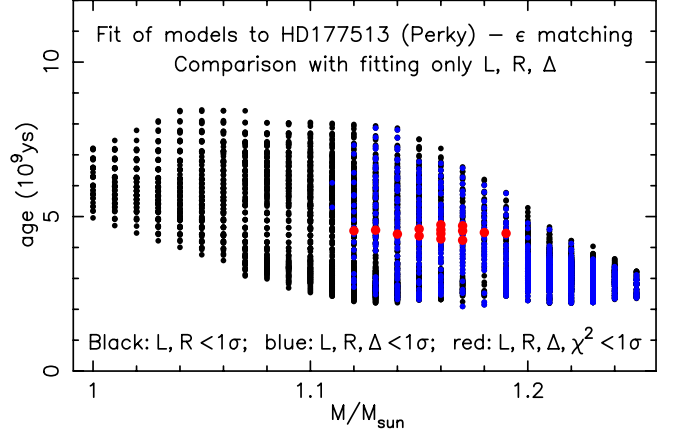


Fig. 10. Models that satisfy different combinations of constraints – models that satisfy all constraints (the large red dots) have $M/M_{\odot} = 1.155 \pm 0.035$ and ages $4.486 \pm 0.250 \times 10^9$ yr.

Table 2. Mass and age for vs fitting criteria $Y \geq 0.255$.

| $\delta L/\sigma_L$ | $\delta R/\sigma_R$ | $\delta \Delta/\sigma_{\Delta}$ | χ^2_{\max} | M/M_{\odot} | age ⁹ |
|---------------------|---------------------|---------------------------------|-----------------|-------------------|-------------------|
| 1 | 1 | 1 | 1.114 | 1.155 ± 0.035 | 4.486 ± 0.250 |
| 1 | ∞ | 1 | 1.114 | 1.145 ± 0.045 | 4.542 ± 0.306 |
| 1 | 1 | ∞ | 1.114 | 1.130 ± 0.060 | 4.546 ± 0.310 |
| 1 | ∞ | ∞ | 1.114 | 1.130 ± 0.060 | 4.622 ± 0.385 |
| ∞ | 1 | 1 | 1.114 | 1.160 ± 0.050 | 4.396 ± 0.548 |
| ∞ | 1 | ∞ | 1.114 | 1.130 ± 0.080 | 4.364 ± 0.629 |
| ∞ | ∞ | 1 | 1.114 | 1.110 ± 0.100 | 4.960 ± 1.112 |
| 1 | 1 | 1 | ∞ | 1.170 ± 0.060 | 4.468 ± 2.376 |
| 1 | 1 | ∞ | ∞ | 1.115 ± 0.115 | 5.094 ± 3.002 |
| 2 | 2 | 2 | 1.535 | 1.110 ± 0.080 | 4.711 ± 0.632 |
| 2 | ∞ | ∞ | 1.535 | 1.115 ± 0.085 | 4.727 ± 0.780 |
| ∞ | 2 | 2 | 1.535 | 1.145 ± 0.125 | 4.371 ± 1.160 |

It is clear from rows 8 and 9 in this table that ϵ matching is needed to narrow down the range of masses and ages. This is clearly illustrated in Fig. 10 where we plot all models that satisfy, to within 1σ , just the constraints on the luminosity and radius (the black points), those that satisfy to within 1σ the constraints on luminosity, radius and large separation (the blue points), and in red the best fit models from Table 1 that also satisfy the epsilon matching constraints.

9. Conclusions

We have shown that if a model and observed star have the same interior structure then their $\epsilon_{\ell}(\nu)$ values, compared at the same frequency reduce to a function only of frequency and not of angular degree ℓ . We then give an algorithm for determining best fit models to an observed frequency set which only requires interpolation in model $\epsilon_{\ell}(\nu_{nl})$ values to determine their values at the observed frequencies, and does not require interpolation in the observed values; as a result the observational errors in the comparison are uncorrelated. We also show that what was once thought to be a possible alternative algorithm, comparing frequencies after subtracting off a best fit function only of frequency, is flawed in principle, gives the same quality of fit for all models with any radii and masses in a family of models which have the same dimensionless structure, and can give erroneous results.

Applying the epsilon matching algorithm to the observed frequency set of HD 177153 (aka Perky) with observational constraints on L , R , Δ we obtain best fit models with masses in the range $1.155 \pm 0.035 M_{\odot}$ and ages in the range $4.486 \pm 0.250 \times 10^9$ yr, which are consistent with the results from phase matching given in Roxburgh (2015a), the 3 best fit models being identical in the two analyses.

Further, on imposing only “pure surface layer independent constraints”, that is only constraints on L and ϵ , we find best fit models with $M/M_{\odot} = 1.13 \pm 0.06$ and age = $4.62 \pm 0.39 \times 10^9$ yr, consistent with the values obtained on imposing a full set of constraints.

Acknowledgements. The author gratefully acknowledges support from the Leverhulme Foundation under grant EM-2012-035/4 and from the UK Science and Technology Facilities Council (STFC) under grant ST/M000621/1.

References

Angulo, C., & the NACRE consortium 1999, *Nucl. Phys. A*, 656, 3
 Ferguson, J. W., Alexander, D. R., Allard, D. T., et al. 2005, *ApJ*, 623, 585

Grevesse, N., & Sauval, A. J. 1998, *Space Sci. Rev.*, 85, 161
 Huber, D., Ireland, M., Bedding, T., et al. 2012, *ApJ*, 760, 32
 Iglesias, C. A., & Rogers, F. J. 1996, *ApJ*, 464, 943
 Kjeldsen, H., Bedding, T. R., & Christensen-Dalsgaard, J. 2008, *ApJ*, 683, L175
 Rauer, H., Catala, C., Aerts, C., et al. 2014, *Exp. Astron.*, 38, 249
 Rogers, F. J., & Nayfonov, A. 2002, *ApJ*, 576, 1064
 Roxburgh, I. W. 2005, *A&A*, 434, 655
 Roxburgh, I. W. 2008a, *Ap&SS*, 316, 75
 Roxburgh, I. W. 2008b, *Ap&SS*, 316, 141
 Roxburgh, I. W. 2009, Presentation at meetings, Synergies between solar and stellar modelling Rome, June 22–26, New Insights into the Sun, the potential of a new generation of solar-stellar diagnostics, Ponte de Lima, Portugal, September 16–18
 Roxburgh, I. W. 2014, *A&A*, 571, A88
 Roxburgh, I. W. 2015a, *A&A*, 574, A45
 Roxburgh, I. W. 2015b, *A&A*, 581, A58
 Roxburgh, I. W., & Vorontsov, S. V. 1994, *MNRAS*, 268, 880
 Roxburgh, I. W., & Vorontsov, S. V. 2000, *MNRAS*, 317, 141
 Roxburgh, I. W., & Vorontsov, S. V. 2003a, *A&A*, 411, 215
 Roxburgh, I. W., & Vorontsov, S. V. 2003b, *Ap&SS*, 284, 187
 Roxburgh, I. W., & Vorontsov, S. V. 2013, *A&A*, 560, A2
 Silva Aguirre, V., Basu, S., Brandao, I. M., et al. 2013, *ApJ*, 769, 17
 van Leeuwen, F. 2007, *A&A*, 474, 653